Supplementary Informaiton

Dual-Phase MoS_2/MXene/CNT Ternary Nanohybrids for Efficient Electrocatalytic Hydrogen Evolution

Sichen Wei,[1] Yu Fu,[1] Maomao Liu,[2] Hongyan Yue,[3] Sehwan Park,[4] Young Hee Lee,[4] Huamin Li,[2*] and Fei Yao[1*]

1 Department of Materials Design and Innovation, University at Buffalo, the State University of New York, Buffalo, NY 14260, USA

2 Department of Electrical Engineering, University at Buffalo, the State University of New York, Buffalo, NY 14260, USA

3 School of Materials Science and Engineering, Harbin University of Science and Technology, Harbin 150040, China.

4 Center for Integrated Nanostructure Physics, Institute for Basic Science, Department of Energy & Department of Physics, Sungkyunkwan University, Suwon, Gyeonggi-do 16419, South Korea.

---

† Corresponding authors: huaminli@buffalo.edu, feiyao@buffalo.edu

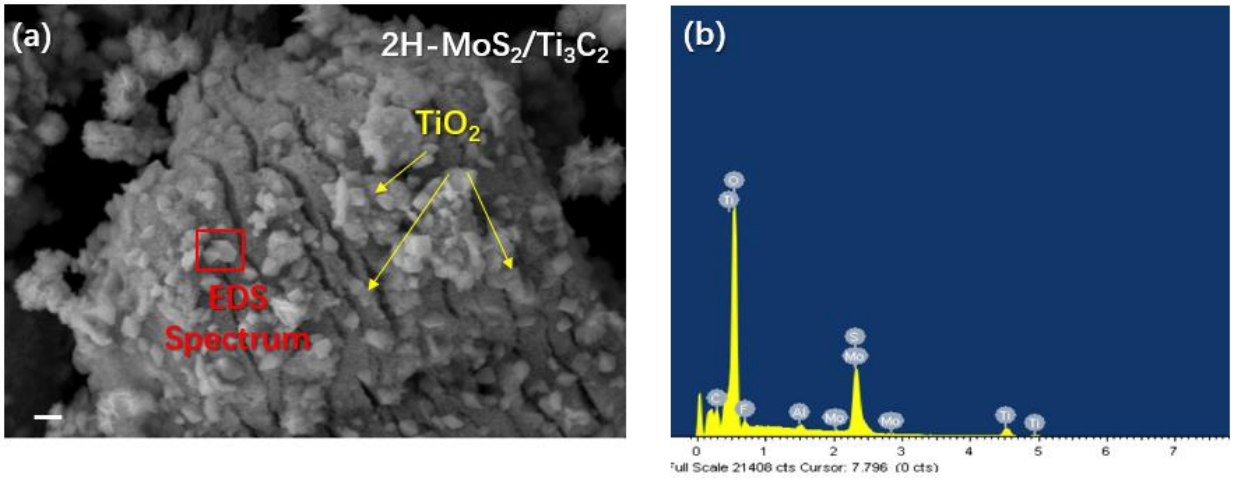

Supplementary Fig. 1 The SEM/EDS of DI-synthesized 2H-MoS_2/Ti_3C_2. (a) The SEM image of aqueous solvent synthesized MoS_2/Ti_3C_2 composite. **(b)** The EDS spectrum taken in the corresponding area marked in **(a)**. Scale bar: 300 nm.

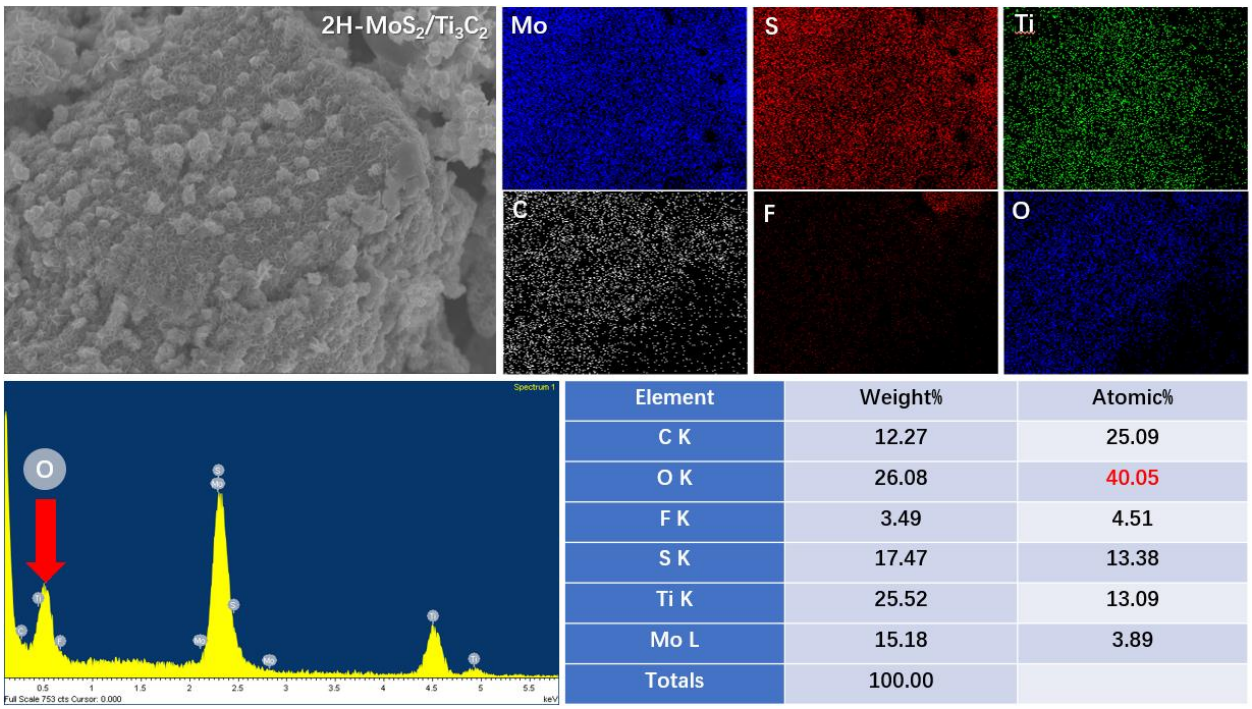

Element	Weight%	Atomic%
C K	12.27	25.09
O K	26.08	40.05
F K	3.49	4.51
S K	17.47	13.38
Ti K	25.52	13.09
Mo L	15.18	3.89
Totals	100.00	

Supplementary Fig. 2 The SEM/EDS of 2H-MoS_2/Ti_3C_2. The SEM image of 2H-MoS_2/Ti_3C_2 and its corresponding EDS mapping and EDS spectrum.

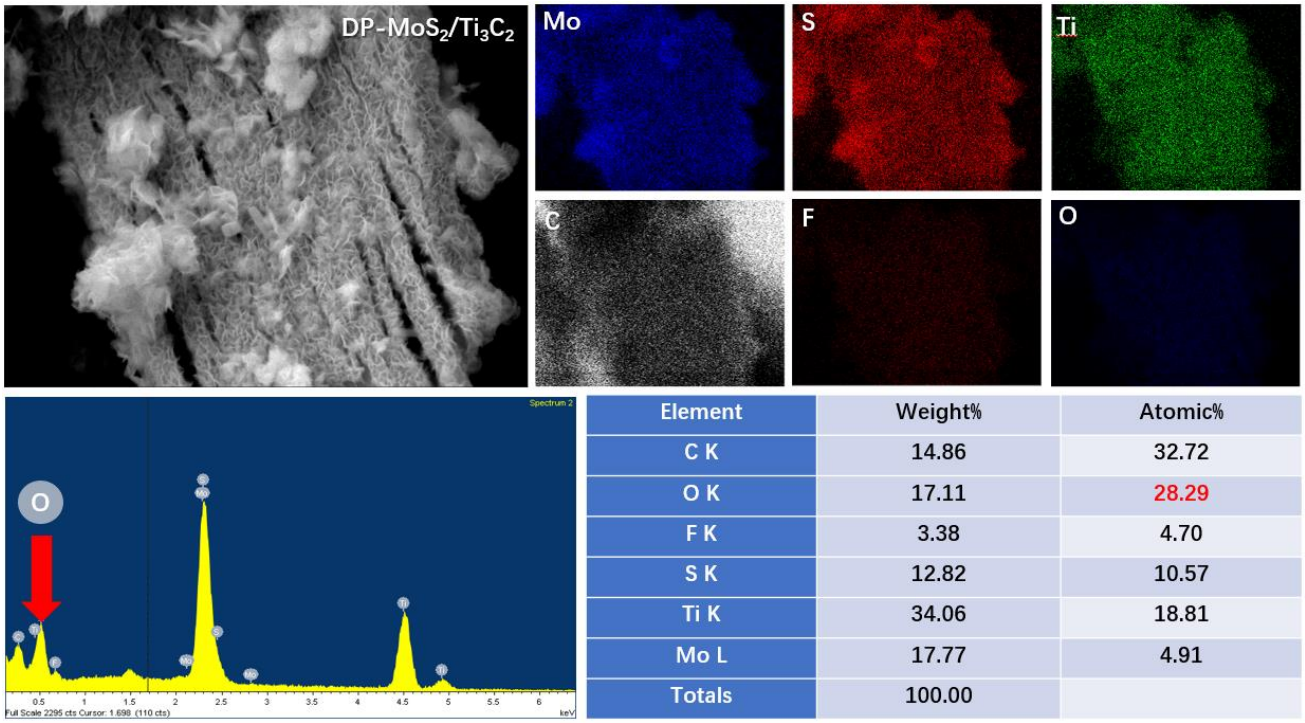

Element	Weight%	Atomic%
C K	14.86	32.72
O K	17.11	28.29
F K	3.38	4.70
S K	12.82	10.57
Ti K	34.06	18.81
Mo L	17.77	4.91
Totals	100.00	

Supplementary Fig. 3 The SEM/EDS of DP-MoS_2/Ti_3C_2. The SEM image of DP-MoS_2/Ti_3C_2 and its corresponding EDS mapping and EDS spectrum.

Supplementary Note 1. Compared with the DI-synthesized MoS_2/Ti_3C_2 composite (see **Supplementary Fig. 1 and 2**), fewer TiO_2 particles along with lower O content were observed in the bisolvent-produced DP-MoS_2/Ti_3C_2, demonstrating successfully suppressed oxidation of MXene during the synthesis process. The low F content was also detected at different locations of the sample due to the introduction of F residual during the Al layer etching process using HCl/LiF, which is corresponding to the XPS analysis in **Fig. 4**. It is worth mentioning that the F content is barely detected in EDS in some locations of the sample due to the detection limit of EDS and the potential nonuniform distribution of the F content in the sample.

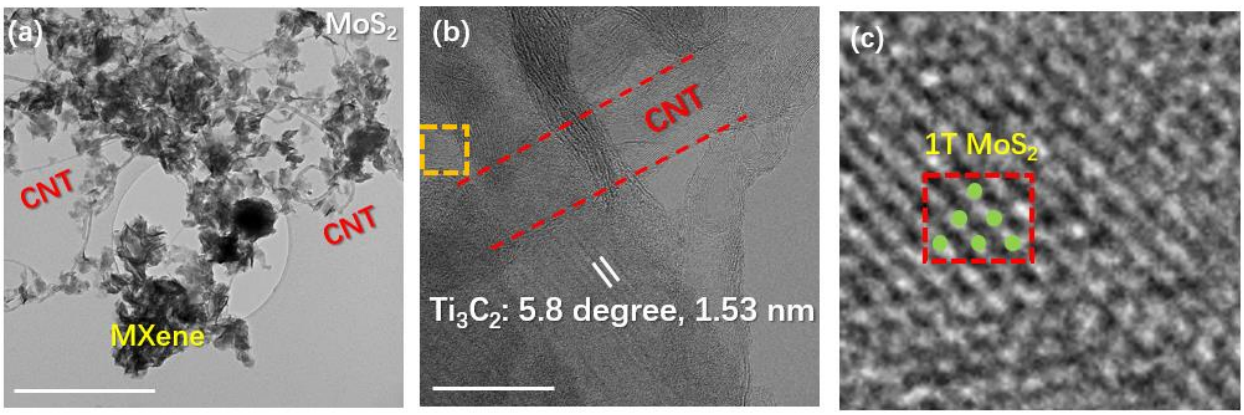

Supplementary Fig. 4 Additional TEM images of MTC hybrid. The TEM image **(a)** and HRTEM image **(b)** of as-synthesized MTC100. The enlarged view of the area marked in the orange box in **(b)** is shown in **(c)**, which clearly shows the 1T phase MoS_2 atom arrangement. Scale bar: **(a)** 1000 nm, **(b)** 20 nm.

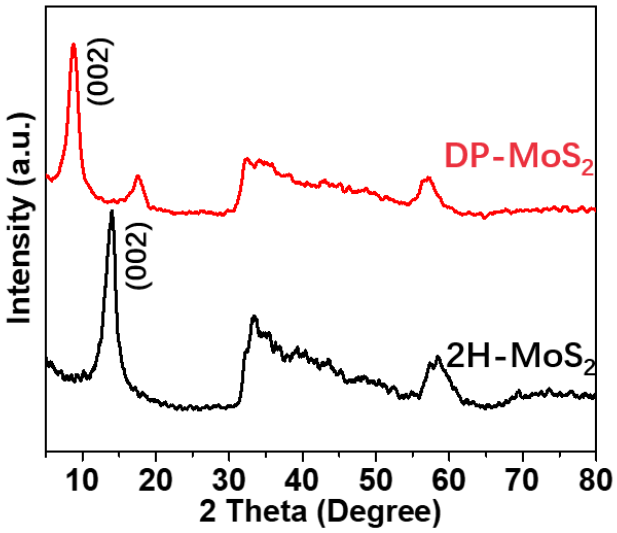

Supplementary Fig. 5 XRD comparison of MoS_2 synthesized in different solvents. The XRD pattern comparison for aqueous synthesized 2H-MoS_2 and as-synthesized DP-MoS_2.

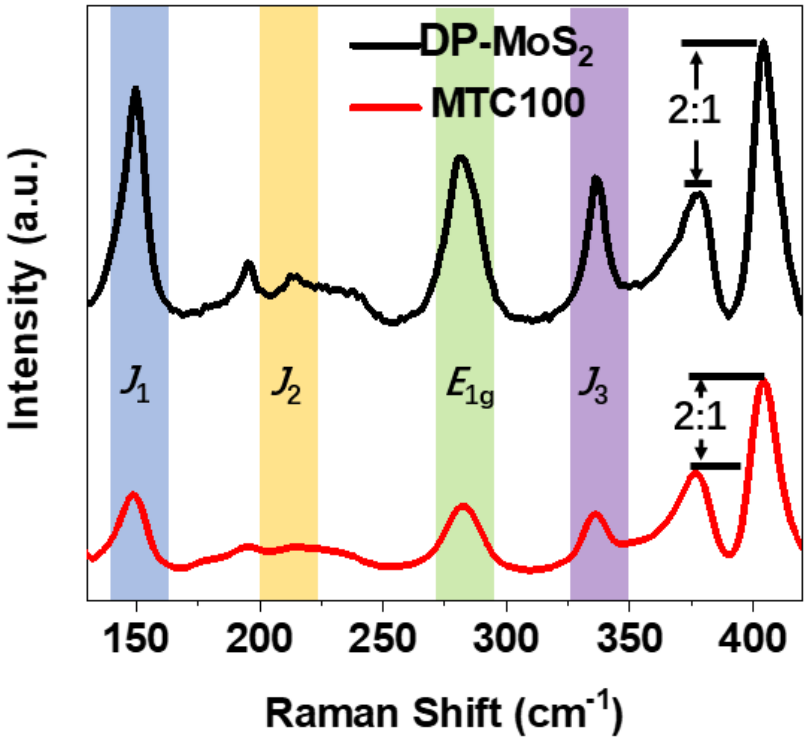

Supplementary Fig. 6 The Raman spectrum highlighting 1T phase MoS_2. The Raman spectra of DP-MoS_2 and MTC100 in order to show the MoS_2 phase features.

Supplementary Note 2. Clear E_{1g} (280 cm^{-1}), E_{2g} (378 cm^{-1}), and A_{1g} (405 cm^{-1}) peaks corresponding to the vibration of atoms along in-plane (E_{1g}, E_{2g}) and out-of-plane (A_{1g}) directions have been detected and are in good agreement with the previous report for 2H-phase MoS_2 [1-3]. On the other hand, the observation of the J_1 (150 cm^{-1}), J_2 (219 cm^{-1}), and J_3 (336 cm^{-1}) phonon modes suggests a clear 1T component in the samples [4-6]. The formation of the 1T phase is a result of NH_4^+ intercalation during the synthesis process, leading to the MoS_2 crystal structure distortion. The existence of the 1T phase in DP-MTC100 is consistent with our HRTEM observation in Supplementary Fig. 4c, where the 1T phase atomic coordination are clearly identified.

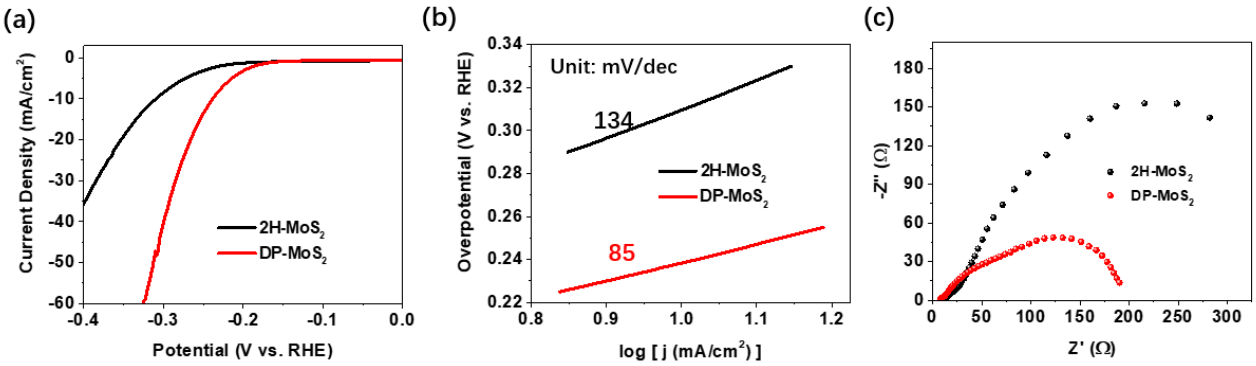

Supplementary Fig. 7 The electrochemical result for 2H and DP-MoS_2. The polarization curve **(a)**, the Tafel plot **(b)**, and the Nyquist plot **(c)** of 2H-MoS_2 and DP-MoS_2.

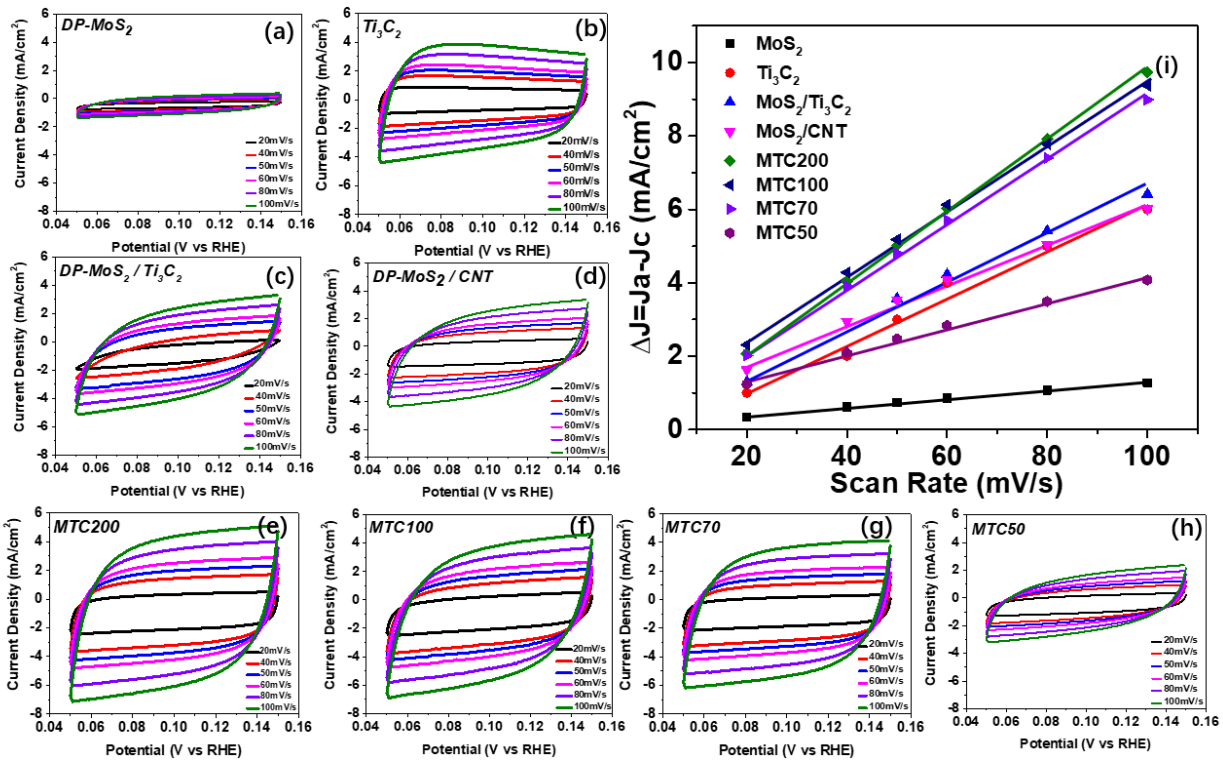

Supplementary Fig. 8 The ECSA results of different samples. The CV curves for different samples tested between -0.3V ~ 0.2V vs. RHE at scan rate of 50 mV/s to determine the electrochemical capacitance are shown in **(a)-(g)**. The corresponding linear fitting of the anodic current density versus scan rate plot is shown in **(i)**.

Supplementary Table 1 The estimated C_{dl} and the corresponding ECSA of different samples.

Sample	C_{dl} (μF/cm^2)	ECSA (cm^2)
Ti_3C_2	36	882
DP-MoS_2	6	144
DP-MoS_2/Ti_3C_2	34	838
DP-MoS_2/CNT	27	676
MTC200	48	1199
MTC100	44	1099
MTC70	43.5	1087
MTC50	18	440

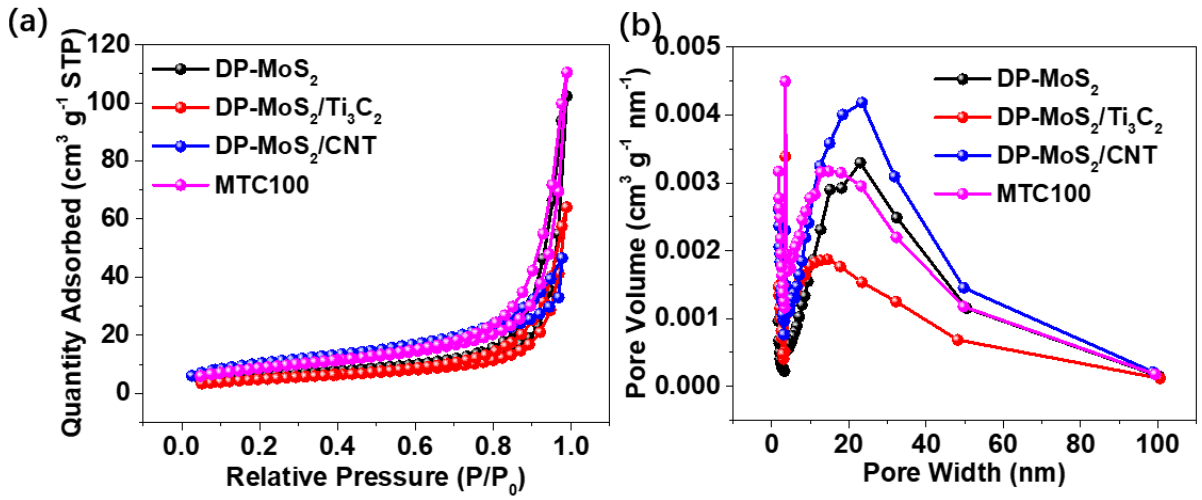

Supplementary Fig. 9 The surface area and pore size characterization. (a) The isotherm N_2 adsorption/desorption curve and **(b)** the pore size distribution of different samples.

Supplementary Reference

1. Zhang, X. et al. Phonon and Raman scattering of two-dimensional transition metal dichalcogenides from monolayer, multilayer to bulk material. *Chem. Soc. Rev*. 44, 2757–2785 (2015).

2. Li, F. et al. Pressure confinement effect in MoS2 monolayers. *Nanoscale* 7, 9075–9082 (2015).

3. Guo, Y. et al. Discovering the forbidden Raman modes at the edges of layered materials. *Sci. Adv.* 4, eaau6252 (2018).

4. Wang, D. et al. Phase engineering of a multiphasic 1T/2H MoS2 catalyst for highly efficient hydrogen evolution. *J. Mater. Chem. A* 5, 2681–2688 (2017).

5. Calandra, M. Chemically exfoliated single-layer MoS2: Stability, lattice dynamics, and catalytic adsorption from first principles. *Phys. Rev. B* 88, 245428 (2013).

6. Nayak, A. P. et al. Pressure-dependent optical and vibrational properties of monolayer molybdenum disulfide. *Nano Lett.* 15, 346–353 (2015)